Optical Properties of Opal and Inverse Opal Infiltrated with Liquid Crystals

Masanori Ozaki, Yuki Shimoda, Ken-ichiro Saisho,

Masahiro Kasano, Hirotaka Miyoshi and Katsumi Yoshino

Department of Electronic Engineering, Graduate School of Engineering, Osaka University

2-1 Yamada-Oka, Suita, Osaka 565-0871, Japan

E-mail: ozaki@ele.eng.osaka-u.ac.jp

Photonic crystals with a three-dimensionally ordered structure with a periodicity of optical wavelength have attracted considerable attention from both fundamental and practical points of view, because novel physical concepts such as photonic band gap have been theoretically predicted and various applications of photonic crystals have been proposed.[1,2] Synthetic opals have been studied as pseudo photonic crystals or prototype photonic crystals to establish growth techniques for the three-dimensional periodic structure. We have already demonstrated that various materials can be infiltrated into interconnected nanosize voids of opals, and novel functionalities can be realized in these infiltrated opals.[3-6] Based on this fabrication technique, a new concept, a tunable photonic crystal, has been proposed, in which the photonic band gap can be tuned as desired by controlling parameters such as the refractive index, periodicity or space filling factor. We have also proposed an anisotropic photonic crystal, in which a three-dimensional periodic array of interconnected voids is infiltrated with anisotropic materials such as liquid crystal (LC).[7,8]

Based on characteristics of LC such as a large optical anisotropy and high sensitivity to an external field, the optical properties of the synthetic opal whose interconnected nano-scale voids are filled with LC should be easily controlled by temperature and electric field.[9-12] In this study we fabricate a silica synthetic opal and a polymer inverse opal (PIO), and demonstrate the tuning of the stop band upon applying electric field in the synthetic opal and the PIO infiltrated with nematic LC.[11,12]

Ordered colloidal crystal was formed by sedimentation of the suspension of mono-dispersed silica spheres in 300-nm diameters in a sandwich cell made of two glass plates with separation of 50μm. The inverse opals were prepared by filling their voids with optically transparent liquid photopolymer (refractive index n=1.56). After polymerization, silica particles were etched in HF. The opal and PIO were infiltrated with nematic LC, 4-pentyl-4'-cyanobiphenyl (5CB) (Merck), in the isotropic phase.

Figure 1 indicates reflection peaks of the opal infiltrated with 5CB as a function of amplitude of applied rectangular voltage (f=1kHz). The light was irradiated perpendicularly to the opal film. As is evident in this figure, the reflection peak shifts to shorter wavelength (blueshift) with increasing voltage. This shift originates from refractive index change caused by the molecular reorientation along applied electric field. In the initial state, the refractive index of the LC in nanosize voids of the opal should be macroscopically averaged and is equivalent to that in the isotropic phase, because of a three dimensional symmetry of the arrangement and shape of the voids without electric field. Under applied electric field, however, the LC molecules align along the field parallel to the direction of the light propagation, and the ratio of the molecules aligning parallel to the light propagation slightly increases. As a result, the component of the refractive index n_o for an ordinary light increases in each voids, and the averaged refractive index of LC decreases. Consequently, the reflection peak shifts to shorter wavelength.
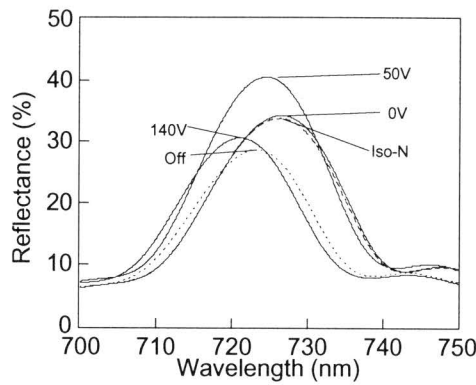
Fig. 1. Reflection spectra of the opal infiltrated with 5CB as a function of applied voltage.
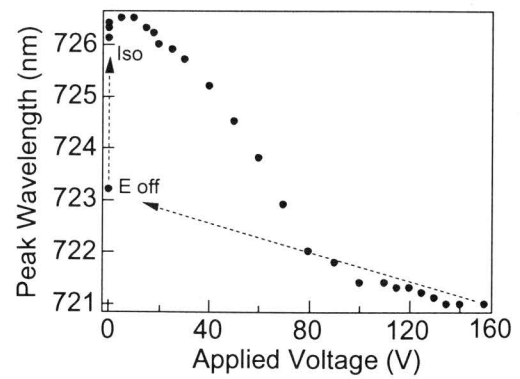

Fig. 2. Applied voltage dependence of the reflection peak wavelength of the opal infiltrated with 5CB

Figure 2 shows the voltage dependence of the reflection peak wavelength of the opal infiltrated with 5CB. As is evident from the figure, reflection peak shifts to shorter wavelength above 10V with increasing applied voltage. The wavelength shift of the reflection peak upon the application of 160V is about 5.5nm, which corresponds to the change in effective refractive index of 0.04 for the infiltrated LC. The refractive indices of 5CB for the ordinary and extraordinary lights of 720nm in wavelength, n_o and n_e, are 1.522 and 1.706, respectively. Assuming a random orientation of the LC molecules in the voids, the averaged refractive index n_{ave} is calculated to be 1.584. If all molecules in the voids completely orient to the electric field, the effective refractive index should change by 0.06 ($= n_{ave} - n_o$).

Figure 3 shows the SEM microphotograph of non-infiltrated PIO. The hexagonal-type close packing of the hollow spherical cavities with small holes connecting the neighboring voids is clearly seen. The wavelength of the reflection maximum for the non-infiltrated PIO λ_v is 533nm.

For the normal incidence geometry, Bragg reflection wavelength λ is determined using following equation,

Fig.3. SEM image of the PIO fabricated with a synthetic opal made of silica spheres of 300nm in diameter.

$$\lambda = 2d\sqrt{fn_v^2 + (1-f)n_p^2} , \qquad (1)$$

where d is the spacing of the (111) planes which is normal to the light propagation direction, f is the filling factor of the fcc close-packed structure, and n_v and n_p are refractive indices of the spherical voids and polymer network in the PIO. In the case of the non-infiltrated PIO, n_v is the refractive index of air. Using f=0.74, n_p=1.56, n_v=1.00 and λ_v=533nm, d is evaluated to be 228nm from eq.(1). This value is smaller (by 7%) than that calculated as $d = \sqrt{2/3}D = 245$nm from the diameter D of silica spheres (D=300nm). As mentioned earlier, the PIO used for LC infiltration is sandwiched between two glass plates and annealed at 60°C for 2 days. As the result, the PIO might be pressed in the [111] direction and d decrease from the original one. In deed, original PIO before annealing procedure has d=241nm, which coincides with the calculated one (d=245nm).

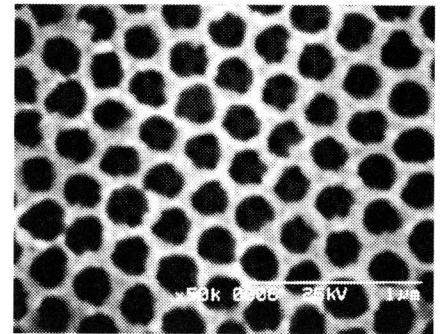Figure 4 shows reflection spectra of the PIO infiltrated with 5CB as a function of amplitude of applied rectangular voltage (1kHz). The light was irradiated perpendicularly to the PIO film, i.e. in the [111]

direction. As is evident from this figure, the reflection peak shifts to shorter wavelength with increasing voltage. Although at lower voltage the peak intensity of the reflection spectrum is suppressed, above V=170V it increases again with increasing voltage. It should also be noted that, around V=150V, two peaks can be observed in the reflection spectrum. This might be attributed to the splitting of the band degeneracy caused by the anisotropy of the LC media.
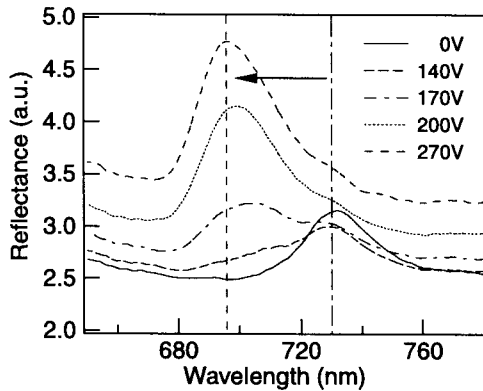

Fig. 4. Reflection spectra of the PIO infiltrated with 5CB as a function of applied voltage.
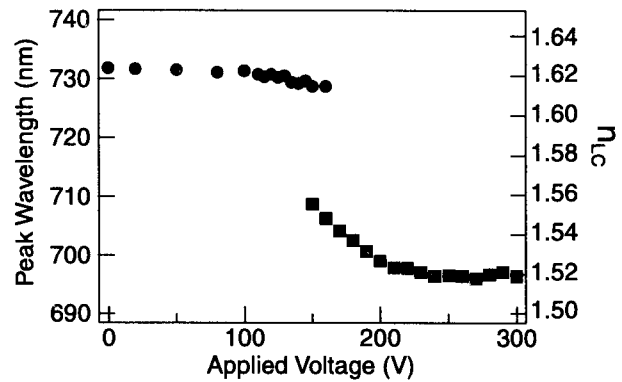
Fig. 5. Applied voltage dependence of the reflection peak wavelength λ_{LC} of the PIO infiltrated with 5CB.

Figure 5 shows the voltage dependence of the reflection peak wavelength λ_{LC} of the PIO infiltrated with 5CB. At lower voltage region ($V < 150V$), λ_{LC} hardly shifts in spit of the increase in voltage. Around V=150V, a clear threshold can be observed and λ_{LC} discontinuously shifts to shorter wavelength with increasing applied voltage. Above the threshold voltage, the peak monotonously blue-shifts and, finally, levels off at voltage higher than 230V. The total shift of λ_{LC} upon the application of 300V is about 35nm, which is much larger than that of the silica opal infiltrated with 5CB as shown in Fig.2. This large peak shift for the PIO should be attributed to the large volume fraction of the voids filled with LC whose refractive index changes upon the voltage application compared with that in the silica opal.

The effective refractive index of LC in the voids n_{LC} has been evaluated assuming fcc closed-pack structure and using n_{LC} for n_v in eq.(1), which is also shown in Fig.3. In the absence of the field, n_{LC} is about 1.62, which coincides with averaged refractive index of the LC whose molecules align in the plane normal to the light propagation, n_{LC}^{2D}. Namely, if all molecules in the voids completely align in the (111) plane, the effective diffractive index is calculated as $n_{LC}^{2D} = \sqrt{(n_e^2 + n_o^2)/2} = 1.617$, where the refractive indices of 5CB for the ordinary and extraordinary lights of 720nm in wavelength, n_o and n_e, are 1.522 and 1.706, respectively. The reason why the averaged molecular orientation is in the (111) plane is as follows. As mentioned above, the PIO used for the LC-infiltration was pressed in the (111) direction. In other words, the voids filling LC should be deformed one-dimensionally. As a result, the optical axis in individual voids orient in the (111) plane and LC molecules align two-dimensionally in the (111) plane.

As shown in Fig.5, above the threshold voltage (V=150V), n_{LC} approaches to 1.52 with increasing voltage, which corresponds to n_o. This means all molecules in the voids completely orient to the electric field. In the case of LC-infiltrated silica opal, the effective refractive index does not coincide with n_o even under the strong electric field of 120kV/cm (Fig.2). This difference between PIO and silica opal might be attributed to the difference of the void's size and the anchoring strength.

It should be noted that the LC infiltrated into PIO exhibits optical memory effect. When the voltage below the threshold (<150V) was applied, reflection spectrum is recovered to the initial state by removing voltage. On the contrary, once the higher voltage than the threshold is applied and the reflection peak largely shifts toward shorter wavelength, it doesn't return back to the initial position even after the removal of applied voltage. This memory effect may originate from the strong anchoring effect in the small voids of the PIO. Especially, the defects of the molecular orientation in the voids generated at the inter-connected channel between neighbored voids might play an important role for the memory effect.

The electrooptic responses of 5CB infiltrated PIO to the applied voltage of a bipolar rectangular waveform (10kHz) was investigated as a function of the voltage amplitude and temperature. It was found that the response time is short comparably to that of a conventional twisted nematic (TN) cell. The origin of the fast response of the nematic LC molecules is not clear at this stage but may be attributed to the deformed non-spherical special shape of the voids. In addition, this non-spherical shape of void having sharp corners and inducing defects of the LC alignment might enhance the acting electric field with respect to the applied field.

Figure 6 indicates the voltage dependence of the rise time at 27°C and 32°C. The rise time is defined as the time required to change the transmission intensity from 10% to 90% of its total change when the bipolar rectangular voltage of 1 kHz is applied. From this figure, it is confirmed that the gradient of voltage vs rise time slope is about −2. That is, the rise time is inversely proportional to square of voltage. This relationship suggests that the optical response of the LC molecules in the voids originates from the dielectric anisotropy. The rise response also depends on the temperature and the response time at 27°C is longer than that at 32°C, which must be associated with the temperature dependence of a viscosity of 5CB.

Fig. 6. Applied voltage dependence of response time to the application of the electric field at 27°C and 32°C.

In summary, we demonstrated that the position of the stop band in the opal and PIO infiltrated with the nematic liquid crystal could be tuned by voltage, which should confirm the possibility of a tunable photonic crystal. It was also found that the discontinuous transition of the λ_{LC} shift upon changing voltage was observed.

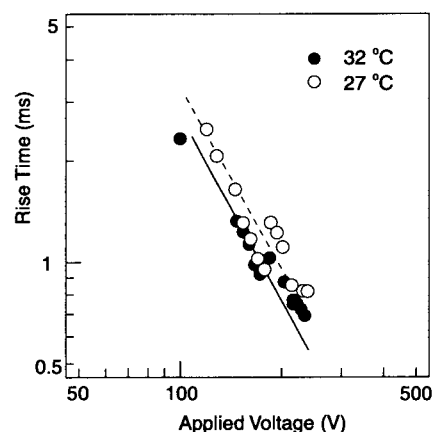[1] S.John, *Phys. Rev. Lett.* **1987**, *58*, 2486,　[2] E.Yablonovitch, *Phys. Rev. Lett.* **1987**, *58*, 2059,　[3] K.Yoshino, K.Tada, M.Ozaki, A.A.Zakhidov, R.H.Baughman, *Jpn. J. Appl. Phys.* **1997**, *36*, L714,　[4] K.Yoshino, S.B.Lee, S.Tatsuhara, Y.Kawagishi, M.Ozaki, A.A.Zakhidov, *Appl. Phys. Lett.* **1998**, *73*, 3506,　[5] K.Yoshino, S.Tatsuhara, Y.Kawagishi, M.Ozaki, A.A.Zakhidov, Z.V.Vardeny, *Jpn. J. Appl. Phys.* **1998**, *37*, L1187,　[6] K.Yoshino, S.Tatsuhara, Y.Kawagishi, M.Ozaki, A.A.Zakhidov, Z.V.Vardeny, *Appl. Phys. Lett.* **1999**, *74*, 2590,　[7] K.Yoshino, *Production & Technique* **1998**, *50*, 26 in Japanese,　[8] K.Busch, S.John, *Phys. Rev. Lett,* **1999**, *83*, 967,　[9] K.Yoshino, Y.Shimoda, Y.Kawagishi, K.Nakayama, M.Ozaki, *Appl. Phys. Lett.* **1999**, *75*, 932,　[10] K.Yoshino, S.Satoh, Y.Shimoda, Y.Kawagishi, K.Nakayama, M.Ozaki, *Jpn. J. Appl. Phys.* **1999**, *38*, L961,　[11] Y.Shimoda, M.Ozaki, K.Yoshino, *Appl. Phys. Lett.* **2001**, *79*, 3627,　[12] M.Ozaki, Y.Shimoda, M.Kasano, K.Yoshino, *Adv.Mater.* **2002**, inpress.